Journal of Luminescence 192 (2017) 653–660

Contents lists available at ScienceDirect

Journal of Luminescence

journal homepage: www.elsevier.com/locate/jlumin

Optical and structural properties of Eu^{2+} doped BaBrI and BaClI crystals

R. Shendrik[a,b,*], A.A. Shalaev[a,b], A.S. Myasnikova[a], A. Bogdanov[a,c], E. Kaneva[a], A. Rusakov[a], A. Vasilkovskyi[a]

[a] Vinogradov Institute of Geochemistry SB RAS, 1a Favorskogo str., Irkutsk 664033, Russia
[b] Physics Department of Irkutsk State University, 20 Gagarina blvd., Irkutsk 664003, Russia
[c] Irkutsk National Researcher Technical University, Lermontov str. 83, Irkutsk 664074, Russia

ARTICLE INFO

Keywords:
Alkali earth halides
Europium
Luminescence
Optical spectroscopy
Ab initio calculation
Scintillators
BaBrI
BaClI

ABSTRACT

The work is necessitated by search for new materials to detect ionizing radiation. The rare-earth doped ternary alkali earth-halide systems are promising scintillators showing high efficiency and energy resolution. Some aspects of crystal growth and data on the structural and luminescence properties of BaBrI and BaClI doped with low concentrations of Eu^{2+} ions are reported. The crystals are grown by the vertical Bridgman method in sealed quartz ampoule. New crystallographic data for BaClI single crystal obtained by single crystal X-ray diffraction are presented. Emission, excitation and optical absorption spectra as well as luminescence decay kinetics are studied under excitation by X-ray, vacuum ultraviolet and ultraviolet radiation. The energies of first 4f-5d transition in Eu^{2+} and band gaps of the crystals are obtained. The electronic band structure of the crystals are calculated using density functional theory as implemented in Vienna *Ab initio* Simulation Package. Calculated band gap energies are in accordance with the experimental estimates. The energy gaps between the valence band maximum and occupied Eu^{2+} 4f levels in BaBrI and BaClI are suggested. In addition, vacuum referred binding energy diagram of lanthanide levels is constructed using the chemical shift model.

1. Introduction

Eu-doped orthorhombic alkali earth halides have recently been utilized as the prospective scintillators for gamma ray detection having high light yield and energy resolution. The strontium iodide crystals doped with Eu^{2+} ions demonstrate excellent properties close to the theoretical limit [1]. This material has been more extensively studied with optical spectroscopy methods within the past decade. Spectroscopic data measured in ultraviolet and vacuum ultraviolet (VUV) regions together with *Ab initio* calculations provide information about exciton and band gap energies [2–5] and are necessary for understanding the mechanism of defect formation and their role in energy transfer.

Recently, the research focus has been shifted to the study of mixed halide compounds due to their superior light yield [6]. In a number of barium dihalides BaFI-BaClI-BaBrI-BaBrCl, the scintillation properties have been studied for Eu-doped BaFI, BaBrCl and BaBrI [7–11]. Despite their excellent properties, experimental data on optical absorption and excitation spectra in spectral region of 4f-5d and band to band transitions are scarce because single-crystals doped with high concentrations of Eu^{2+} ions (more than 5 mol%) were used. When measuring high concentration doped samples, the inner filter effects can be observed. These include reabsorption and non uniform excitation throughout the sample. These effects dramatically change the shape of excitation spectrum. Therefore, estimation of the lowest energy of 4f-5d transitions in Eu-doped BaBrI given in [10,8] could be incorrect. Furthermore, the experimental determination of band gap in these crystals is not possible due to high absorption related to allowed $4f^7 \rightarrow 4f^6 5d^1$ transitions in Eu^{2+} ions. At this moment, band gap energies of the mixed halide compounds are based on theoretical estimates.

We investigate luminescence, electrical and structural properties of undoped BaBrI, BaBrI-0.05 mol% Eu^{2+} and BaClI-0.1 mol% Eu^{2+} crystals. Absorption, excitation and emission spectra, photoluminescence decay time constants, dielectric properties and pulsed height spectra are presented. The vacuum referred binding (VRBE) energy diagram is constructed based on density functional calculations. The diagram shows the electron binding energy in the ground and excited state levels of all divalent and trivalent lanthanides ions in BaBrI and BaClI crystals.

2. Methodology

2.1. Growth and structural characterization

The crystals were grown by the vertical Bridgman method in sealed

* Corresponding author at: Vinogradov Institute of Geochemistry SB RAS, 1a Favorskogo str., Irkutsk 664033, Russia.
E-mail address: r.shendrik@gmail.com (R. Shendrik).

http://dx.doi.org/10.1016/j.jlumin.2017.07.059
Received 7 April 2017; Received in revised form 21 July 2017; Accepted 28 July 2017
Available online 29 July 2017

quartz ampoules in vacuum. The temperature gradient was about 10–15 °C/cm, and the growth rate was 1 mm/hour. The reagents used for the growth were $BaBr_2$, BaI_2 and $BaCl_2$ (purity 99.9%, Lanhit, LTD). The stoichiometric mixtures of $BaBr_2 + BaI_2$ and $BaCl_2 + BaI_2$ were employed. The samples were doped with of $EuBr_3$ and $EuCl_3$, respectively. Because the material is hydroscopic, the batch was thoroughly dried prior to sealing the ampoule of diameter 10–30 mm. The melting points, the level of hydration and the possible dehydration temperatures of the charge materials were determined by thermogravimetric and differential scanning calorimetry methods prior to the crystal growth. The melting points for BaBrI and BaClI are about 783 °C and 815 °C, respectively.

The plates about 1–2 mm of thickness and 1 cm in diameter were cut and polished in glove box for optical absorption and luminescence spectra measurements. The rest of grains were analyzed to determine structure. For pulse height spectra measurements, a sample $1 \times 1 \times 1$ cm^3 of BaClI-0.1 mol% Eu^{2+} was cut, polished and coated with polytetrafluoroethylene (PTFE) tape to maximize the light collection efficiency.

The diffraction patterns of grown BaBrI crystals were in agreement with the early published data in Ref. [10]. We report the new data for BaClI single crystal measured by single crystal X-ray diffraction method. Structure analysis of BaClI crystals was carried out using a Bruker AXS D8 VENTURE dual source diffractometer with a Photon 100 detector under monochromatized Mo-K_α radiation. Low temperature data was acquired with the crystal cooled by a Bruker Cobra nitrogen Cryostat. Three sets of 20 frames were utilized for initial cell determination, whereas complete data were collected by several φ and ω scans with 0.3^o rotation, 2 s exposure time per frame and crystal-to-detector distance 40 mm. The data collection strategies were optimized by the APEX2 program suite [12], and the reflection intensities were extracted and corrected for the Lorentz-polarization by the SAINT package [13]. A semi-empirical absorption correction was applied by means of the SADABS software [14]. It was revealed that the studied samples crystallize in orthorhombic symmetry. The XPREP software assisted in the determination of the space group (*Pnma*) and in calculation of intensity statistics. Finally, the least-squares refinements were performed by the program CRYSTALS [15]. The structures were resolved with the use of the charge flipping algorithm [16], and the space group was confirmed by the analysis of the reconstructed electronic density.

Scale factors, atomic positions, occupancies and atomic displacement factors were the refined parameters. In preliminary anisotropic refinement the R values converged to $R \approx 4$.

The obtained unit cell parameters are: $a = 8.4829(5)$, $b = 4.9517(3)$, $c = 9.6139(5)$ Å, $V = 403.83$ Å^3. The density of BaClI crystals calculated from the structure is 4.94 g/cm^3. In the orthorhombic *Pmna* structures of studied crystals the Ba, Cl and I atoms occupy fourfold special positions (4c) and lie on the mirror planes, perpendicular to the b axis. Barium atom position is coordinated by 9 anions with mean interatomic distances: Ba-Cl ~3.15 and Ba-I ~ 3.59 Å(Fig. 1). X-ray powder diffraction data were obtained by diffractometer D8 ADVANCE Bruker in range of diffraction angles 2θ varying from 3 to 80°, CuK_α radiation. The experimental conditions were the following: 40 kV, 40 mA, time per step − 1 s and step size − 0.02^o, Goubel mirror. The XRD pattern of the sample is shown in Fig. 1 and is similar to that obtained in Ref. [17]. However, we obtain the space group *Pnma* in contrast to the *Pbam* reported in Ref. [17].

2.2. Optical and dielectric characteristic measurements

The optical absorption spectra were obtained by a Perkin-Elmer Lambda 950 UV/VIS/NIR spectrophotometer at 300 K. Photoluminescence (PL) was measured in vacuum cold-finger cryostat. The spectra were recorded with a MDR2 and SDL1 (LOMO) grating monochromator, a photomodule Hamamatsu H6780-04 (185–850 nm), and a photon-counter unit. The luminescence spectra were corrected for spectral response of detection channel. The photoluminescence excitation (PLE) spectra were measured with a grating monochromators MDR2 and 200 W xenon arc lamp for direct 4f-5d excitation and vacuum monochromator VM-2 (LOMO) and Hamamatsu deuterium lamp L7292 for measurements in VUV spectral region. The PLE spectra were corrected for the varying intensity of exciting light due. Photoluminescence decay curves were registered by an oscilloscope Rigol 1202 under pulse nitrogen laser excitation with impulse duration about 10 ns. The X-ray excited luminescence was performed using an X-ray tube operating at 50 kV and 1 mA.

The measurements of pulse height spectra were carried out with a photomultiplier tube Enterprises 9814QSB. The PMT was operated with a CSN638C1 negative polarity voltage chain. The focusing system of 46 mm active diameter was assumed to be 100% photoelectron collection efficiency in the center of the photocathode. The sample was irradiated with gamma rays from a monoenergetic γ-ray source of ^{137}Cs (662 KeV). A homemade preamplifier and an Ortec 570 amplifier were used to obtain pulse height spectra. The samples are optically coupled to the window of PMT using mineral oil.

The dielectric constant of the BaBrI crystal was measured using immitance meter E7-20 manufactured by MNIPI. The measurements of capacitance and dielectric losses were performed in frequency range from 25 Hz to 1 MHz. The silver paint (kontaktol “Kettler”) was employed as the electrode contact material. The pad area was about 60 mm^2 and the sample thickness was about 1 mm. To prevent surface degradation the dieletric measurements of polished samples were made in the glove box.

2.3. Calculation details

*A*b Initio calculations of BaClI crystal doped with Eu^{2+} were carried out within density functional theory (DFT) using VASP (Vienna *Ab initio* Simulation Package) computer code [18]. Using the unit sell parameters from the X-ray diffraction we constructed the $2 \times 2 \times 1$ (48 atoms) supercell, in which one of Ba^{2+} ions was replaced by Eu^{2+}.

The spin-polarized calculations were carried out within the framework of the generalized gradient approximation (GGA) with the exchange-correlation potential PBE [19]. Integration within the Brillouin zone was performed on a Γ-centered grid of 8 irreducible k points. Geometry optimization was performed with fixed cell dimensions. The convergence was achieved if the difference in total energy between the two last iterations was less than 10^{-6} eV.

3. Results and discussion

3.1. Eu^{2+} luminescence

Figs. 2 and 3 show the absorption spectra for Eu^{2+} ions in BaBrI and BaClI crystals measured at room temperature and the relative emission and excitation spectra measured at 80 K. Strong absorption bands are observed from $4f^7$ ground state to $4f^65d^1$ states in both figures (curves 1). The maxima of peaks are 280 (4.43 eV) and 292 nm (4.25 eV) for BaBrI crystal and 278 (4.46 eV) and 290 nm (4.25 eV) for BaClI crystal.

The excitation wavelength for the emission is 290 nm. At this wavelength, the optical penetration depth is less than 1 mm for all the samples. The emission spectra, which result from 5d-4f transitions with peaks at 415 nm (2.99 eV) in BaBrI-Eu and 410 nm (3.02 eV) in BaClI-Eu (curves 3 in Figs. 2 and 3), agree well with previously published data [10,17].

The excitation spectra of 5d-4f emission of BaBrI-Eu and BaClI-Eu crystals monitored at 415 and 410 nm (curves 2 in Figs. 2 and 3) agree well with the optical absorption spectra.

The ground state of Eu^{2+} ions includes seven 4f electrons, which, according to the Hund's rules, give rise to the ground state $^8S_{7/2}$. The bands consist of two clearly distinguishable peaks and slightly expressed characteristic “staircase” structure. In BaBrI and BaClI crystals

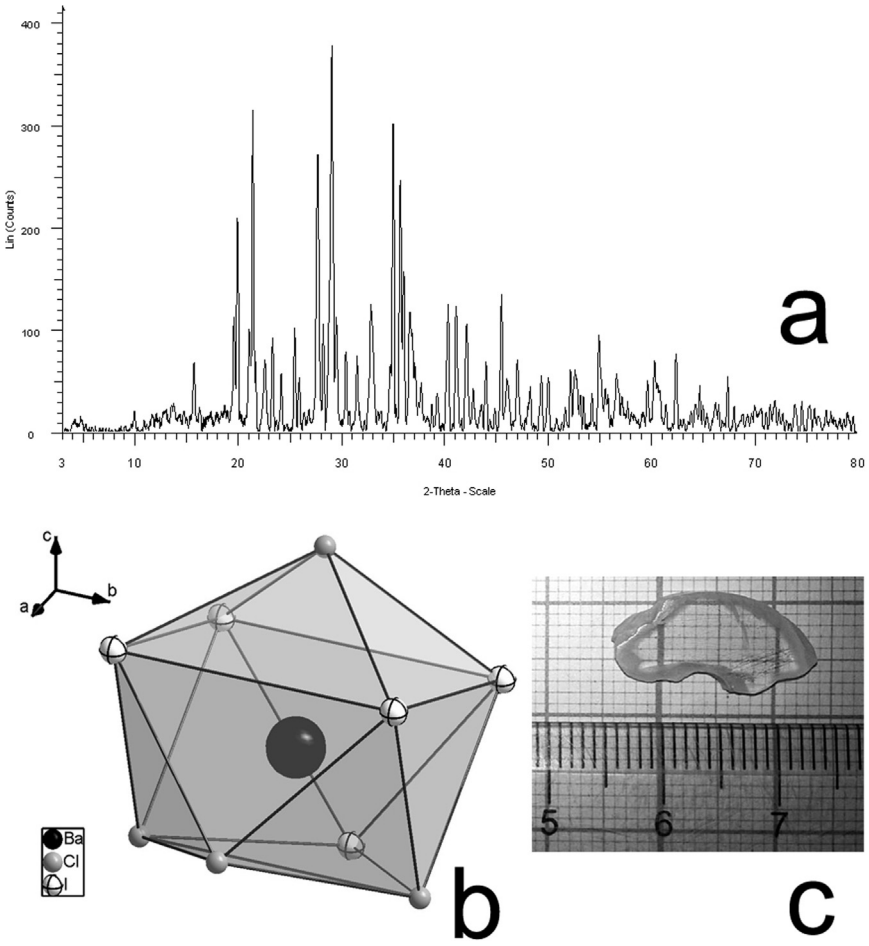

Fig. 1. (a) X-ray diffraction spectrum of powder BaClI sample. (b) Arrangement of Cl and I anions around each Ba atom. (c) Photograph of the BaClI-0.1 mol% Eu^{2+} crystal.

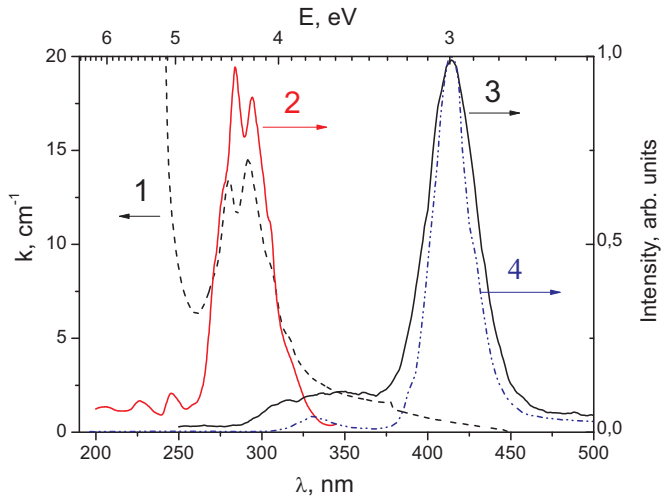

Fig. 2. Optical absorption (dashed curve 1), excitation (curve 2) monitored at 415 nm, and emission spectra under intracenter 4f-5d excitation at 290 nm (curve 3) and x-ray excitation (dot curve 4) of BaBrI crystals doped with 0.05 mol% Eu^{2+} ions.

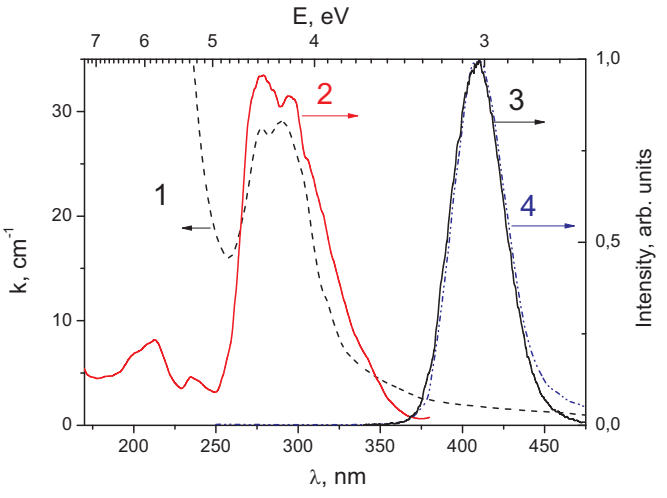

Fig. 3. Optical absorption (dashed curve 1), excitation (curve 2) monitored at 410 nm, and emission spectra under intracenter 4f-5d excitation at 290 nm (curve 3) and x-ray excitation (dot curve 4) of BaClI crystals doped with 0.1 mol% Eu^{2+} ions.

the site symmetry of cations is D_{2h} as found in structure determination experiment. In D_{2h} symmetry the degeneracy of the t_{2g} is lifted and the t_{2g} level splits into three levels. Excitation and absorption spectra indicate two bands corresponding to a t_{2g} level splitting into three levels, where degeneracy of two of them is weak. The characteristic "staircase" structure was originally explained by transitions from the $^8S_{7/2}$ to the seven ^7F_J multiplets (J = 0–6) of the excited $4f^6(^7F_J)\,5d^1$ configuration [20]. It is feasible to the lowest energy of 4f-5d transtion (λ_{abs}) from the absorption spectra for BaBrI-Eu and BaClI-Eu. According to P. Dorenbos [20], this value pertains to the first step of the characteristic "staircase" structure in 4f-5d absorption and excitation spectra of Eu^{2+} corresponding to the zero phonon-line in emission spectrum, such as Ca F_2 doped Eu^{2+} ions [21]. Usually "staircase" structure and vibronic structure of Eu^{2+} emission band are not resolved. Therefore, the λ_{abs} value is estimated on the energy of low-energy side, where the band has risen to 15–20% of the maximum of the "staircase". In this method

some level of arbitrariness may introduce an error. To keep the errors small, the data on samples with low Eu concentration were preferably used. In previous works [22], the estimation of λ_{abs} 397 nm is based on the measurement of crystals doped with high concentrations of Eu^{2+} ions (more than 5 mol%). Excitation spectra of the samples of BaBrI doped with higher concentrations of Eu^{2+} ions are given in Figure in Supplementary. The spectra are different from those shown in the Fig. 2 in that they exhibit a dip in the region of the Eu^{2+} absorption maximum. Thus, excitation spectra could not be measured correctly due to self-absorption. Therefore, λ_{abs} value contains a large error. From absorption spectra of BaBrI-0.05 mol% Eu^{2+} and BaClI-0.1 mol% Eu^{2+} we found λ_{abs}(BaBrI) = 376 nm for BaBrI – Eu^{2+} and λ_{abs}(BaClI) = 373 nm. The lowest energies of 4f-5d transition in Eu^{2+} ion are 3.29 eV for BaBrI and 3.32 eV for BaClI.

At all temperatures the investigated crystals show only strong 5d-4f luminescence and no 4f–4f emission. At room temperature Eu^{2+} compounds can exhibit broad and strong fluorescence resulting from the 5d-4f transitions, as well as sharp line emission, which has been assigned to 4f–4f transitions from $^6P_{7/2}$ to $^8S_{7/2}$ terms. The presence of both 5d-4f and 4f–4f transitions indicates the proximity of the lowest excited 5d and the $4f^7$ ($^6P_{7/2}$) states. The relative positions of the 5d and $^6P_{7/2}$ levels change in different hosts. Strong 5d-4f band emission is observed when the lowest 5d state is significantly lower than the $^6P_{7/2}$ level, f-f sharp line emission appears when the reverse is true. Both 5d-4f and f-f bands in luminescence spectrum are obtained when the energy of the levels are close. Decreasing temperature causes to redistribution of intensities 4f–4f and 5d-4f luminescence lines. Increase of 4f–4f luminescence and the corresponding reduction of 5d-4f luminescence at low temperatures take place, when the lowest 5d state lies slightly above $^6P_{7/2}$ terms of 4f state. That type of luminescence was observed in Eu^{2+} doped BaFCl and SrFCl crystals [21]. Energy of $^6P_{7/2}$ level in relation to the ground $^8S_{7/2}$ level is about 3.49 eV. Thus, it can be concluded that the energy 5d state in relation to $^8S_{7/2}$ level is significantly lower than 3.49 eV. Therefore, our estimation of the lowest 4f-5d energies should be reliable.

Luminescence decay curves measured at the maximum of the emission peak under nitrogen laser excitation at 337 nm are mono-exponential in shape (Fig. 4). The measured time constants of the photoluminescence decay kinetics were equal to τ = 390 ns for BaClI-Eu (Fig. 4 curve 1) and τ = 400 ns for BaBrI-Eu (Fig. 4) crystals. The values are quite similar to the time-constants obtained with other types of excitations [10,9].

BaBrI and BaClI crystals doped with Eu^{2+} ions demonstrate bright luminescence under x-ray and gamma-ray excitation. The spectra of x-ray excited luminescence are given in curves 4 in Figs. 2 and 3. The spectra are in agreement with photoluminescence spectra. The X-ray

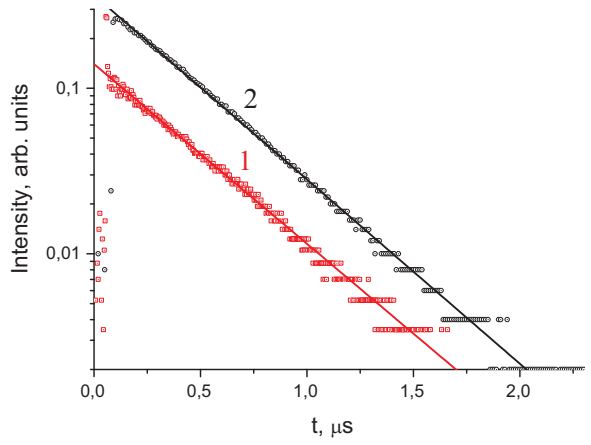

Fig. 4. Luminescence decay curves of BaClI-0.1 mol% Eu^{2+} (curve 1) and BaBrI-0.05 mol % Eu^{2+} (curve 2) excited at 337 nm.

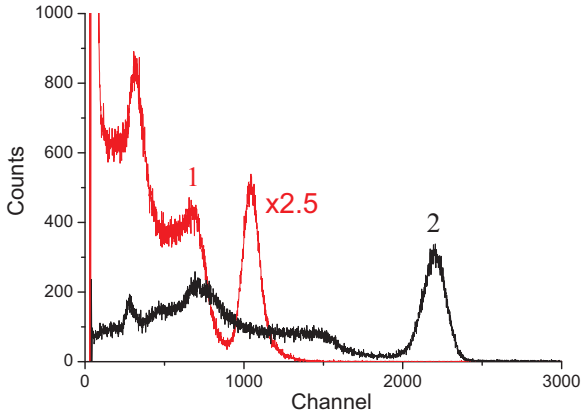

Fig. 5. Pulsed-height spectra of BaClI-0.1 mol% Eu^{2+} and NaI-Tl (light output is about 41,000 photons/MeV [24]).

excited luminescence output measured by integral intensity is compared with the one of CaF_2-Eu crystal. Light output of CaF_2-Eu crystals is approximately 21,000 photons/MeV [23,24]. Therefore, the light output of measured samples can be estimated. BaBrI doped with 0.05 mol% Eu has light output about 25,000 photons/MeV. Light output of BaClI doped with 0.1 mol% Eu^{2+} is estimated about 30,000 photons/MeV. Authors obtained [7,25] 97,000 photons/MeV light output in BaBrI doped with 5–7% Eu^{2+} ions. Therefore, we can expect to increase light output in the crystals with higher than 0.1 mol% concentrations of Eu^{2+} ions.

Light output of BaClI-Eu calculated from the pulsed height spectrum (Fig. 5) is about 9000 photons/MeV and energy resolution is about 11%. This value is much lower than the one obtained from the x-ray excited luminescence spectra. The spread is attributed to various factors. The first one is the lower optical quality of large crystal with respect to quality of the small sample used in the x-ray luminescence spectra measurements. The other reason consists in possible presence of intensive slow components in Eu^{2+} x-ray and gamma excited luminescence similar to [23,26].

3.2. Exciton emission and band gap

In the X-ray excited luminescence spectra of the Eu-doped samples we observe a low intensity peak at higher energy (about 3.8–4 eV) together with intense Eu attributed luminescence. In nominally undoped BaBrI crystals this luminescence dominates, and its intensity increases at low temperatures (Fig. 6, curve 3). Under VUV excitation we also observe the same emission. The instensity of luminescence decreases with concentration of Eu^{2+} ions and it is almost absent at 0.1 mol.% and higher Eu^{2+} concentrations. In BaClI we also obtain luminescence band in the 300–320 nm spectral region. The inset of Fig. 7 contains the luminescence spectra under excitation to 4f-5d Eu^{2+} band (curve 2) and VUV excitation at about 165 nm. The spectra look different. Under VUV excitation the additional relatively weak bands appear at about 300–320 nm and 460–520 nm. The excitation spectra of the luminescence centered at 320 nm in undoped and doped with 0.05 mol.% Eu^{2+} BaBrI crystals are shown in Fig. 6 in comparison with optical absorption spectra. In all samples the most efficient photoluminescence excitation ranges from about 5.1–5.7 eV and lies within interband absorption spectrum.

The excitation spectrum of 300–320 nm emission band in BaClI-0.1 mol% Eu crystal is provided in Fig. 7. Similarly to BaBrI crystals a narrow peak is found in fundamental absorption region. The observed luminescence is attributed to self-trapped excitons (STE). As it was first shown by Hayes and confirmed by Song and Williams [27,28] the STE in alkaline-earth fluorides consists of molecular ion similar to H-center (hole on interstitial fluorine) and an F-center-like part (electron trapped

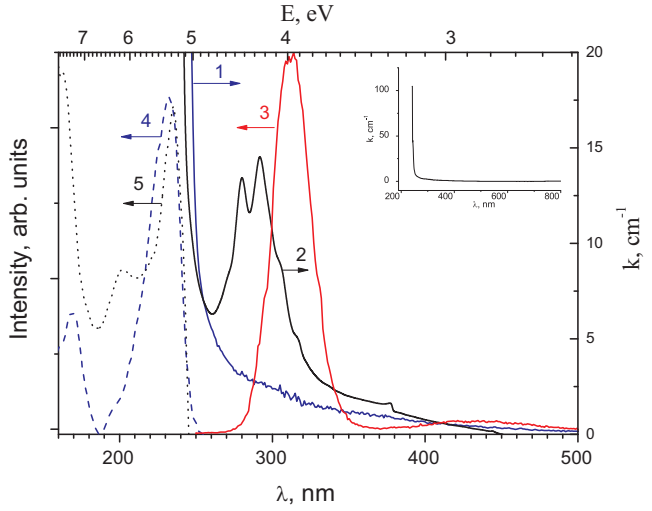

Fig. 6. Optical absorption spectra of undoped (curve 1) and 0.05 mol% Eu^{2+} doped BaBrI. The inset contains absorption spectra of undoped BaBrI. Emission spectrum of pure BaBrI measured at 78 K corresponds to curve 3 under X-ray and interband (at about 161 nm) excitations. Dashed curve 4 and dotted curve 5 are excitation spectra at 320 nm emission wavelength in the undoped and Eu-doped crystals, respectively.

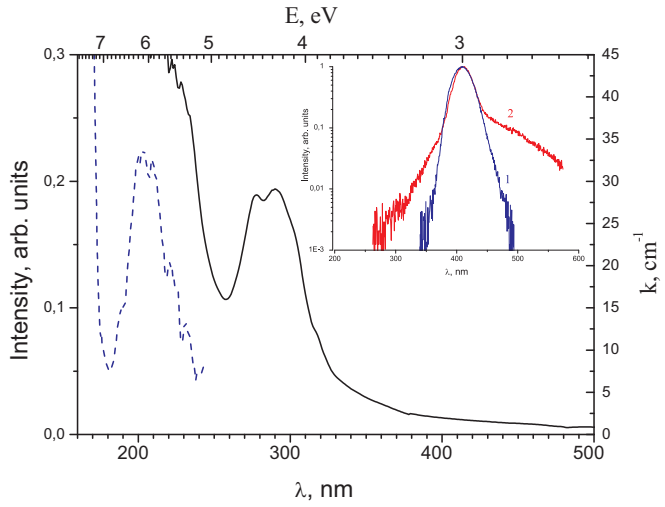

Fig. 7. Excitation spectrum of at 320 nm emission wavelength (dashed curve) measured at 77 K in comparison with absorption spectrum of BaClI-0.1 mol% Eu^{2+} (solid curve). The inset displays emission spectra under 290 nm (curve 1) and interband (curve 2) excitations.

fluorine vacancy). Radzhabov pointed out that STE in barium dihalides has the configuration similar to the excitons in alkali-earth fluorides [29]. In SrI_2 crystal with close band gap the alike emission was also ascribed to self-trapped exciton emission [4,3]. The STE luminescence quenching with Eu^{2+} concentration is due to the exciton emission and 4f-5d Eu^{2+} absorption spectra overlapping, which makes possible a resonant transfer from exciton to Eu^{2+} ions.

Emission peaked at 480 nm and excited at about 245–250 nm can be attributed to oxygen-vacancy centres. This oxygen related emitting center has also been identified and discussed in the other alkali earth metal halides, such as BaFCl and BaFBr [30] and in SrI_2 [2,3]. This luminescence has previously been suggested to be the STE luminescence [9]. Pustovarov [2] concluded that a significant part of the oxygen contamination comes from the surface hydrate reactions in strontium iodide and similar mechanism can take place in the investigated crystals. The oxygen luminescence in contrast to the exciton emission is quenched at low temperatures similarly to the other barium dihalides [31,30].

To estimate exciton binding energy we need to measure the dielectric constant of the crystals. The dieletric constant (ε′) is calculated using measured capacitance at different frequencies. The value of ε′ at 1 MHz is about 9.93 ± 0.2.

Assuming hydrogen like energy levels for a simple exciton model, the exciton binding energy is plotted as function of 1 s hydrogen-like wave function, then its Bohr radius a_0^*. Let assume that the variation of $m = m^*$ is relatively small in the considered ionic crystals (BaFBr, BaFI, KBr, RbI, NaI, CaF_2, Sr F_2, Ba F_2). Therefore, considering the Ref. [32], we can suppose that exciton binding energy:

$$E_b = \frac{e^2}{\varepsilon' a_0^*} = \frac{e^2}{(m^*/m)a_0(\varepsilon')^2} = \frac{E_0}{(m^*/m)(\varepsilon')^2}, \quad (1)$$

where $m(m^*)$ is electron (effective reduced) mass, ε′ is the dielectric constant of material, a_0 is the Bohr radius for the hydrogen atom, E_0 = 13.6 eV is the ionization energy of hydrogen atom, and e is the electron charge.

To estimate exciton binding energy in BaBrI and BaClI we plot exciton binding energies versus dielectric constants for a set of known materials. Exciton binding energies for KBr, RbI and NaI are known from Refs. [33–35]. The binding energies of CaF_2, Sr F_2, and Ba F_2 were obtained in [36]. The energies for BaFBr and BaFI crystals measured in Ref. [37] are 0.66 and 0.32 eV, respectivelly. The dielectric constants for BaFBr and BaFI are 6.14 and 8.8 following by [38]. It is evident from Fig. 8 that proposed model quite correctly describes delocalized excitons created under interband excitation at the initial time in ionic crystals. In this model, the n-th level (n = 1,2,3,…) of the exciton energy E_x is expressed as [39]:

$$E_x = E_g - \frac{E_b}{n^2}, \quad (2)$$

where E_g is the band gap of crystal and E_b is exciton binding energy. Because the model above gives a good agreement between dielectric constants and binding energies for diverse crystals, we can conclude that the primary process is excitation of conduction electrons and valence holes or directly free exciton. The next step is rapid localisation into a self-trapped exciton (STE). It is clear that this model can not be applied to the STE.

Considering the spread of values for the crystals, it is possible to estimate exciton binding energy in BaBrI crystal as 0.23 ± 0.02 eV. Exciton energy (E_x) corresponds to the exciton peak in Figs. 6, 7. It can be determined following the procedure proposed by Ref. [40]. The exciton energies are about 5.35 ± 0.15 eV for BaBrI and 6.0 ± 0.4 eV for BaClI. Therefore, the band gap of the crystal is obtained by adding

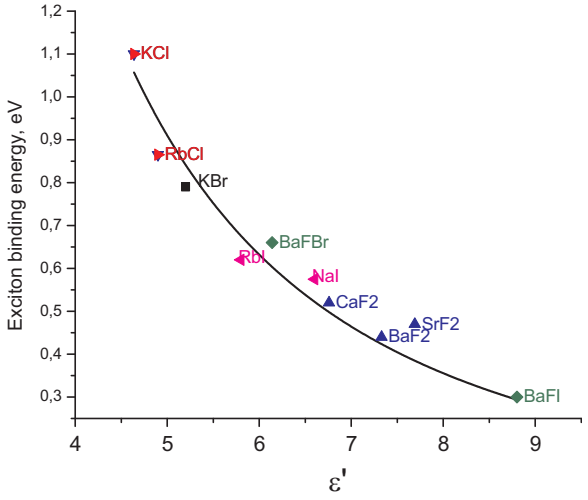

Fig. 8. Dependence of an exciton binding energy (E_b) on dielectric constant for various ionic crystals. Solid line fits the curve following Eq. (1) $E_b = 22.75/(\varepsilon')^2$.

1 s exciton energy to the exciton binding energy (Eq. (2)). The one is E_g = 5.58 ± 0.17 eV for BaBrI. This value is smaller than the one estimated from Dorenbos empirical rule $E_g = 1.08 \cdot E_x$ [41]. The 1.08 proportionality factor was determined as the average of the limited available data. The error on the location of the conduction band depends on the type of anions in material. For most of iodides this rule gives less than 68% prediction interval [42].

We did not measure dielectric constant for BaClI, nevertheless we suppose that the dielectric constant value lies between 8.8 (ε′ (BaFI)) and 9.91 (ε′ (BaBrI)). We use the value 9.35, that is the mean in the interval 8.8 and 9.9, as dielectric constant of BaClI for exciton binding energy estimation. Therefore, exciton binding energy in BaClI is about 0.26 ± 0.05 eV and band gap of BaClI is about 6.26 ± 0.3 eV.

3.3. Calculation results

Electronic structures of Eu-doped BaBrI and BaClI were calculated in order to estimate the location of Eu^{2+} 5d and 4f levels in the band gap of the crystals. The ground state of Eu^{2+} ion configuration $[Xe]4f^7$ is characterized by a half-filled 4f shell. In Refs. [22,43] it was shown that a correct description of the 4f electrons requires adding an effective on-site Coulomb interaction between f-electrons (characterized by the Hubbard U value). Therefore, the Dudarev's approximation PBE + U [44] was applied to correct the positions of 4f levels. In accordance with literature U_{eff} for Eu^{2+} doped wide gap materials should be ≥ 4 [45,46]. However, authors of Ref. [22] showed that the most correct Eu^{2+} 4f levels described with U_{eff} from 2.2 to 2.5.

Some methodological calculations of BaBrI: Eu^{2+} crystals were performed to identify U_{eff} value for the method. The results of the calculations are almost identical to the ones obtained in Ref. [22]. The value U_{eff} was chosen to be 2.5, which gave a good agreement with the data reported in Ref. [22] ((4f-VBM = 1.4 eV) for BaBrI: Eu^{2+}). The calculated 4f-VBM gap for BaClI: Eu^{2+} was 1.5 eV at U_{eff} = 2.5.

The band gap was estimated both by the PBE, and by the GW_0 approximations [47,48]. Using of PBE density functional calculations leads to excess delocalisatin of electronic states in semiconductors and dielectrics and underestimate the energy of the band gap [49]. However, the GW_0 method gives more accurate values for band gaps in ionic crystals, comparable with the experimental data [22,43,49]. The results of our calculations are presented in Table 1. Finally, we can estimate the energy of 5d-CBM transition using the calculated band gap and 4f-VBM energy, and experimental data of the first 4f → 5d transtion. The estimated 5d-CBM values were 0.65 and 0.75 eV for BaBrI: Eu^{2+} and BaClI: Eu^{2+} and agreed well with the data obtained in Ref. [22].

The calculation of the excited state of $[Xe]4f^65d^1$ configuration of Eu^{2+} ion was performed by setting the occupancy of the highest 4f state to zero. The isosurface of electron density for the excited state of Eu^{2+}-doped BaClI is shown in Fig. 9. The $5d^1$ excited state is almost completely localized on the Eu ion for both investigated crystals.

3.4. Vacuum referred binding energy diagram of the lanthanide ions in BaBrI and BaClI

Behaviour of spectroscopic properties of the lanthanide ions can be predicted with respect to their ionic charge and number of electrons into 4f-shell. The energy diagrams are plotted for BaBrI and BaClI crystals based on the experimental values of band gap, exciton creation and 4f-5d transition energies and calculated position of ground state of Eu^{2+} relative to the top of the valence band obtained in this work. The diagram shows the binding energies of an electron in the divalent and trivalent lanthanide ion ground and excited states (Fig. 10). By using the Dorenbos chemical shift model [50], these binding energies are related to the binding energy of an electron at rest in vacuum defined as zero of energy (Vacuum Referred Binding Energy (VRBE) diagram).

Table 1
Calculated band gaps and relative 4f and 5d levels for Eu^{2+}-doped BaBrI and BaClI crystals. Energies are given in eV.

Crystal	Band gap			Eu^{2+},	Eu^{2+},	Eu^{2+},
	PBE	GW_0	Exp.	4f – VBM	4f → 5d	5d – CBM
BaBrI	3.49	5.34	5.58 ± 0.17	1.4	3.29	~ 0.65
BaClI	3.71	5.57	6.26 ± 0.3	1.5	3.32	~ 0.75

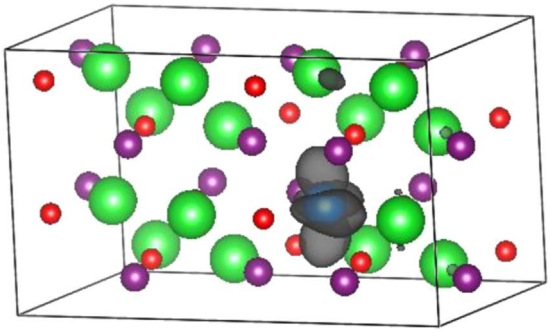

Fig. 9. Isosurface of the electron density for the Eu^{2+} first excited state of BaClI: Eu^{2+}. Eu atom is shown in blue, Ba – in green, Cl – in mangenta, I – in red. (For interpretation of the references to color in this figure legend, the reader is referred to the web version of this article.)

We do not have spectrocopic data about trivalent lanthanides in the investigated crystals, therefore the Coulomb repulsion energy $U(6, A)$ is used. It defines the binding energy difference between an electron in the ground state of Eu^{2+} with that in the ground state of Eu^{3+} [51,52]. U (6,A) energy is chosen not only as an average value in between that typical for iodide and chloride crystals. If band gap and gap between 4f level and top of valence band are known the VRBE of bottom of conduction band can be estimated using U(6,A). BaBrI and BaClI crystals differ only in the anion sublattices, so we can expect that the values of the energy of the bottom of the conduction band should be close in these crystals and they are not significiantly exceed the vacuum energy. Whereas the top of valence band in BaClI crystal should have larger negative VRBE than in BaBrI. Similarly to the other alkali-earth iodide and bromide compounds like $LaBr_3$ and SrI_2 it is estimated as 6.4 eV for BaBrI.

In consideration of chlorides have higher $U(6, A)$ energy, the $U(6, A)$ is estimated as 6.9 eV for BaClI. This immediately defines the VRBE of electrons in the $4f^n$ states of divalent and trivalent lanthanides. The calculated energies between the top of the valence band and Eu^{2+} ground state in BaBrI are about 1.4 eV and 1.5 eV in BaClI crystals (see Table 1). Energies of the top of valence band E_v are equal to − 5.18 and − 5.7 eV for BaBrI and BaClI, respectivelly. Using exciton creation energy E_x (5.35 ± 0.15 eV for BaBrI and 6.0 ± 0.4 eV) and exciton binding energy E_b (0.23 eV for BaBrI and 0.26 eV for BaClI) the energies of conduction band bottom (E_c) are calculated. There are about 0.4 eV in BaBrI and 0.53 eV in BaClI. These values are above the vacuum level implying that BaBrI and BaClI should be a negative electron affinity material ($E_C > 0$, $\chi = -E_C$). The fact, that $E_C > 0$, can be explained by uncertainty in measurements of exciton creation and binding energies and an error in calculation of distance between Eu^{2+} ground state and top of valence band. On the other hand, the chemical shift model gives negative electron affinity $\chi = -0.6$ eV for some materials such as LiCaAlF$_6$, $SrAl_{12}O_{19}$ and SrI_2 due to the model limitations [52,53,5].

Following the diagrams, the ground states of divalent La, Ce, Gd, and Tb ions are to be 4f5d. Stable divalent La, Ce, Gd, and Tb ions and accompanying them photochromic centres can exist as pointed in Refs. [54,55]. The divalent state of these ions can be obtained by x-ray irradiation or additive coloration in alkali-earth metal vapours.

It is clear from the diagrams in Fig. 10 that all 4f ground levels of trivalent rare earth ions excluded Ce^{3+} lie deeply in valence band.

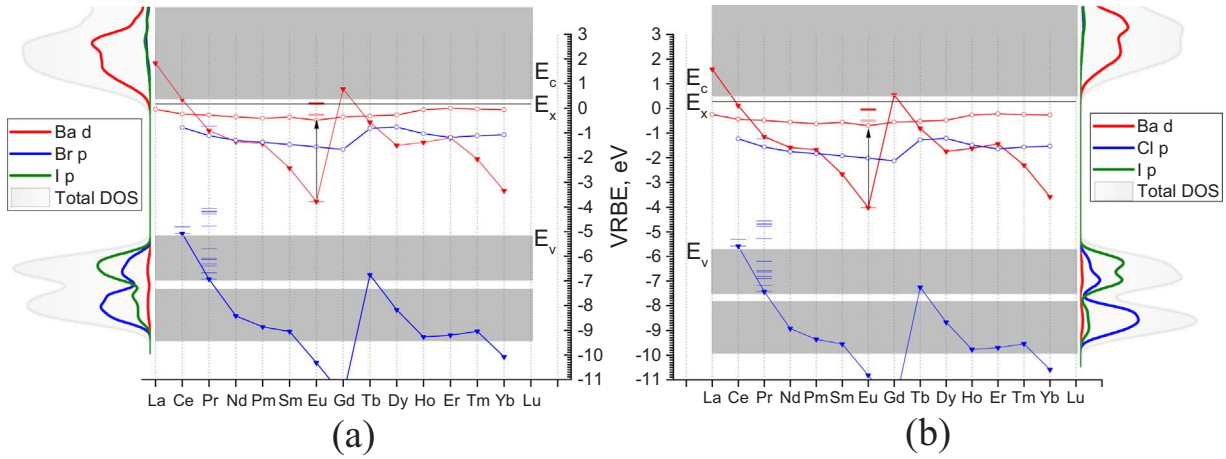

Fig. 10. The diagram shows the vacuum referred binding energies (VRBE) for electrons of divalent (red) and trivalent (blue) lanthanide ions with respect to the vacuum level in BaBrI (a) and BaClI (b). The zigzag red curve with triangles connects the $4f^n$ ground state energies of the divalent lanthanide ions. The red curve with circles is attributed to their lowest $4f^{n-1}$ $5d^1$ states. Blue zigzag curve with triangles respects to $4f^n$ ground state energies of trivalent lanthanide ions and blue curve with circles are their $4f^{n-1}$ $5d^1$ states. Arrow shows the energy of 4f-5d transition measured in this work. The left and right insets provide the calculated density of states (DOS) for BaBrI and BaClI crystals, accordingly. (For interpretation of the references to color in this figure legend, the reader is referred to the web version of this article.)

Therefore, we expect only 4f–4f luminescence from the trivalent rare earth dopants in these crystals. In constrast, the ground 4f and 5d levels of Ce^{3+} ions are in band gap and 5d-4f luminescence in the Ce^{3+} doped crystals can be possible.

The alkali-earth fluorides are not efficient scintillators despite of the Ce^{3+} and Pr^{3+} 5d-4f luminescence. The reason for this is the inefficient energy transfer from “hot” holes in valence band to rare-earth ions. The energy barrier for hole capturing by the rare earth ion is higher than the energy of hole self-trapping. Therefore, in alkali-earth fluorides energy is transferred through hole traps to rare earth ion. This leads to hyperbolic law of the luminescence decay and low light yield [26]. If the ground state of trivalent rare earth ion is located closer to the top of valence band then probability of hot hole capturing increases. The ground state of Ce^{3+} in BaClI and BaBrI crystals is located close to the top of valence band as predicted from the chemical shift model. Therefore, Ce-doped BaClI and BaBrI crystals would be promising scintillators with high light output.

Notwithstanding, 5d-4f luminescence is possible for trivalent lanthanide ions having ground state lower than top of valence band. Theoretical calculations indicate that valence band of the investigated crystals consists of two subbands formed by p-orbitals of iodine and bromine or chlorine ions (Fig. 10, left and right insets). The iodine valence band lies upper than the bromine and chlorine as well as in BaFBr and BaFCl crystals where valence band is formed by bromine-fluorine and chlorine-fluorine subbands [37,56]. Ground state of oxygen-vacancy centres in BaFBr and BaClI crystals is located within valence band in gap between the subbands whereas excited states are located in band gap. Bright luminescence related to the oxygen-vacancy centres was observed [30]. Therefore, if a ground state of lanthanide ion is found in the gap between the subbands, then 5d-4f luminescence is observed. According to the calculations, the ground state of Pr^{3+} is located into the gap. In this case 5d-4f luminescence is observed in Pr-doped BaBrI and BaClI crystals inasmuch as the lowest 5d state is lower than $4f(^1S_0)$ level. The efficient hole capture by the Pr-ions is expected. In Pr-doped alkali-earth fluorides the high temperature stability of light yield was demonstrated in Ref. [57]. We are looking forward to the same effect for Pr-doped BaClI and BaBrI crystals. Thus, on basis of the predictions of the chemical shift model, Ce^{3+} and Pr^{3+} ions seem to be promising activators for the scintillation BaClI and BaBrI crystals.

4. Conclusion

The BaClI and BaBrI single crystal undoped and doped with 0.05–0.1 mol% Eu^{2+} ions were grown. The scintillation, luminescence and structural properties of BaBrI and BaClI crystals doped with low concentrations of Eu^{2+} ions have been studied. The structure of BaClI crystals was determined by single-crystal X-ray diffraction technique. The results obtained by luminescence spectroscopy revealed the presence of divalent europium ions in the BaBrI and BaClI crystals.

The intense bands in absorption and excitation spectra, having slightly manifested characteristic “staircase” structure peaked at about 4.25–4.4 eV for BaBrI and 4.25–4.45 eV for BaClI crystals, result from $4f^7(^8S_{7/2}) \rightarrow 4f^6 5d^1(t_{2g})$ transitions. The lowest energies of 4f-5d transition in Eu^{2+} ion obtained from the spectra were 3.29 eV for BaBrI and 3.32 eV for BaClI. The narrow intense peaks at 5.35 and 6 eV in the photoluminescence excitation spectrum of the intrinsic emission of BaBrI and BaClI crystals were due to the creation of excitons. The band gaps of BaBrI and BaClI crystals were estimated about 5.58 and 6.26 eV consequently using hydrogen-like exciton model.

The band gap was estimated using the PBE and GW_0 approximations. The calculated band gap energies agree with the experimental data. The distance between the lowest 5d level of Eu^{2+} ions and top of the valence band has been calculated. The VRBE diagrams of levels of all divalent and trivalent lanthanides ions in BaBrI and BaClI crystals were constructed on the acquired experimental and theoretical data.

Acknowledgments

This work was partially supported by RFBR Grant 15-02-06514a. The reported study was performed with the equipment set at the Centres for Collective Use (”Isotope-geochemistry investigations” at A.P. Vinogradov Institute of Geochemistry SB RAS and “Analysis of organic state” at A.E. Favorsky Institute of Chemistry SB RAS). Authors acknowledge facilities of Information and Computing Center of NSU as well as HPC cluster Academician V.M. Matrosov at Irkutsk Supercomputer Centre of SB RAS and Academician V.A. Fock supercomputer at Irkutsk National Research Technical University.

Appendix A. Supplementary data

Supplementary data associated with this article can be found in the online version at http://dx.doi.org/10.1016/j.jlumin.2017.07.059.

References

[1] E.V. van Loef, C.M. Wilson, N.J. Cherepy, G. Hull, S.A. Payne, W.-S. Choong,

W.W. Moses, K.S. Shah, Crystal growth and scintillation properties of strontium iodide scintillators, IEEE Trans. Nucl. Sci. 56 (3) (2009) 869.
[2] V. Pustovarov, I. Ogorodnikov, A. Goloshumova, L. Isaenko, A. Yelisseyev, A luminescence spectroscopy study of scintillation crystals SrI_2 doped with Eu^{2+}, Opt. Mater. 34 (5) (2012) 926–930.
[3] V. Pankratov, A.I. Popov, L. Shirmane, A. Kotlov, G.A. Bizarri, A. Burger, P. Bhattacharya, E. Tupitsyn, E. Rowe, V.M. Buliga, Luminescence and ultraviolet excitation spectroscopy of SrI_2 and SrI_2:Eu^{2+}, Radiat. Meas. 56 (2013) 13–17.
[4] I. Ogorodnikov, V. Pustovarov, A. Goloshumova, L. Isaenko, A. Yelisseyev, V. Pashkov, A luminescence spectroscopy study of SrI_2: Nd^{3+} single crystals, J. Lumin. 143 (2013) 101–107.
[5] M.S. Alekhin, R.H. Awater, D.A. Biner, K.W. Krämer, J.T. de Haas, P. Dorenbos, Luminescence and spectroscopic properties of Sm^{2+} and Er^{3+} doped SrI_2, J. Lumin. 167 (2015) 347–351.
[6] E. Bourret-Courchesne, G. Bizarri, R. Borade, G. Gundiah, E. Samulon, Z. Yan, S. Derenzo, Crystal growth and characterization of alkali-earth halide scintillators, J. Cryst. Growth 352 (1) (2012) 78.
[7] E. Bourret-Courchesne, G. Bizarri, S. Hanrahan, G. Gundiah, Z. Yan, S. Derenzo, BaBrI:Eu^{2+}, a new bright scintillator, Nucl. Instrum. Methods Phys. Res. Sect. A: Accel. Spectrometers Detect. Assoc. Equip. 613 (1) (2010) 95.
[8] G. Gundiah, E. Bourret-Courchesne, G. Bizarri, S.M. Hanrahan, A. Chaudhry, A. Canning, W.W. Moses, S.E. Derenzo, Scintillation properties of Eu^{2+} -activated barium fluoroiodide, IEEE Trans. Nucl. Sci. 57 (3) (2010) 1702.
[9] G. Bizarri, E.D. Bourret-Courchesne, Z. Yan, S.E. Derenzo, Scintillation and optical properties of BaBrI:Eu^{2+} and $CsBa_2I$:Eu^{2+}, IEEE Trans. Nucl. Sci. 58 (6) (2011) 3403–3410.
[10] G. Gundiah, G. Bizarri, S.M. Hanrahan, M.J. Weber, E.D. Bourret-Courchesne, S.E. Derenzo, Structure and scintillation of Eu $^{2+}$-activated solid solutions in the BaBr $_2$-BaI $_2$ system, Nucl. Instrum. Methods Phys. Res. Sect. A: Accel. Spectrometers Detect. Assoc. Equip. 652 (1) (2011) 234–237.
[11] Z. Yan, T. Shalapska, E. Bourret, Czochralski growth of the mixed halides BaBrCl and BaBrCl:Eu, J. Cryst. Growth 435 (2016) 42–45.
[12] Bruker, APEX2, Bruker AXS Inc., Madison, Wisconsin, USA.
[13] Bruker, SAINT, Bruker AXS Inc., Madison, Wisconsin, USA.
[14] G. Sheldrick, Sadabs, Program for Empirical Absorption Correction of Area Detector Data, University of Göttingen, Göttingen, Germany.
[15] P.W. Betteridge, J.R. Carruthers, R.I. Cooper, K. Prout, D.J. Watkin, Crystals version 12: software for guided crystal structure analysis, J. Appl. Crystallogr. 36 (6) (2003) (1487–1487).
[16] L. Palatinus, G. Chapuis, Superflip-a computer program for the solution of crystal structures by charge flipping in arbitrary dimensions, J. Appl. Crystallogr. 40 (4) (2007) 786–790.
[17] A.J. Lenus, D. Sornadurai, K.G. Rajan, B. Purniah, Luminescence behaviour of Eu^{2+}-doped bacli and babri, Mater. Lett. 57 (3) (2002) 635–638.
[18] G. Kresse, J. Hafner, Ab initio molecular dynamics for liquid metals, Phys. Rev. B 47 (1) (1993) 558.
[19] J.P. Perdew, K. Burke, M. Ernzerhof, Generalized gradient approximation made simple, Phys. Rev. Lett. 77 (18) (1996) 3865.
[20] P. Dorenbos, Energy of the first $4f^7 \rightarrow 4\ f^6 5d$ transition of Eu^{2+} in inorganic compounds, J. Lumin. 104 (4) (2003) 239–260.
[21] T. Kobayasi, S. Mroczkowski, J.F. Owen, L.H. Brixner, Fluorescence lifetime and quantum efficiency for 5d → 4f transitions in Eu^{2+} doped chloride and fluoride crystals, J. Lumin. 21 (3) (1980) 247–257.
[22] A. Chaudhry, R. Boutchko, S. Chourou, G. Zhang, N. Grønbech-Jensen, A. Canning, First-principles study of luminescence in Eu^{2+}-doped inorganic scintillators, Phys. Rev. B 89 (15) (2014) 155105.
[23] R. Shendrik, E. Radzhabov, A. Nepomnyashchikh, Scintillation properties of pure and Ce^{3+}-doped SrF_2 crystals, Radiat. Meas. 56 (2013) 58–61.
[24] R. Shendrik, E. Radzhabov, Absolute light yield measurements on SrF_2 and BaF_2 doped with rare earth ions, IEEE Trans. Nucl. Sci. 61 (1) (2014) 406–410.
[25] E. Bourret-Courchesne, G. Bizarri, R. Borade, G. Gundiah, E. Samulon, Z. Yan, S. Derenzo, Crystal growth and characterization of alkali-earth halide scintillators, J. Cryst. Growth 352 (1) (2012) 78–83.
[26] R. Shendrik, E. Radzhabov, Energy transfer mechanism in Pr-doped SrF_2 crystals, IEEE Trans. Nucl. Sci. 59 (5) (2012) 2089–2094.
[27] K. Song, R.T. Williams, Self-Trapped Excitons, Springer Science & Business Media, Vol. 105, 2013.
[28] J. Beaumont, W. Hayes, D. Kirk, G. Summers, An investigation of trapped holes and trapped excitons in alkaline earth fluorides, in: Proceedings of the Royal Society of London A: Mathematical, Physical and Engineering Sciences, The Royal Society, vol. 315, 1970, pp. 69–97.
[29] E. Radzhabov, A. Egranov, Exciton emission in BaFBr and BaFCl crystals, J. Phys.: Condens. Matter 6 (29) (1994) 5639.
[30] E. Radzhabov, V. Otroshok, Optical spectra of oxygen defects in BaFCl and BaFBr crystals, J. Phys. Chem. Solids 56 (1) (1995) 1–7.
[31] E. Radzhabov, Time-resolved luminescence of oxygen-vacancy centres in alkaline-earth fluoride and barium fluorohalide crystals, J. Phys.: Condens. Matter 6 (45) (1994) 9807.
[32] M. Dvorak, S.-H. Wei, Z. Wu, Origin of the variation of exciton binding energy in semiconductors, Phys. Rev. Lett. 110 (1) (2013) 016402.
[33] J. Ramamurti, K. Teegarden, Intrinsic luminescence of RbI and KI at 10 °K, Phys. Rev. 145 (2) (1966) 698.
[34] R. Williams, M. Kabler, Excited-state absorption spectroscopy of self-trapped excitons in alkali halides, Phys. Rev. B 9 (4) (1974) 1897.
[35] Y. Onodera, Y. Toyozawa, Excitons in alkali halides, J. Phys. Soc. Jpn. 22 (3) (1967) 833–844.
[36] T. Tomiki, T. Miyata, Optical studies of alkali fluorides and alkaline earth fluorides in VUV region, J. Phys. Soc. Jpn. 27 (3) (1969) 658–678.
[37] E. Nicklaus, Optical properties of some alkaline earth halides, Phys. Status Solidi A 53 (1) (1979) 217–224.
[38] D. Ayachour, M. Sieskind, P. Geist, Electrical properties of alkaline earth fluorohalide crystals, Phys. Status Solidi B 166 (1) (1991) 43–52.
[39] T. Tsujibayashi, M. Watanabe, O. Arimoto, M. Itoh, S. Nakanishi, H. Itoh, S. Asaka, M. Kamada, Resonant enhancement effect on two-photon absorption due to excitons in alkaline-earth fluorides excited with synchrotron radiation and laser light, Phys. Rev. B 60 (12) (1999) R8442.
[40] A. Belsky, J. Krupa, Luminescence excitation mechanisms of rare earth doped phosphors in the VUV range, Displays 19 (4) (1999) 185–196.
[41] P. Dorenbos, The Eu^{3+} charge transfer energy and the relation with the band gap of compounds, J. Lumin. 111 (1) (2005) 89–104.
[42] J.J. Joos, D. Poelman, P.F. Smet, Energy level modeling of lanthanide materials: review and uncertainty analysis, Phys. Chem. Chem. Phys. 17 (29) (2015) 19058–19078.
[43] A. Canning, A. Chaudhry, R. Boutchko, N. Grønbech-Jensen, First-principles study of luminescence in Ce-doped inorganic scintillators, Phys. Rev. B 83 (12) (2011) 125115.
[44] S. Dudarev, G. Botton, S. Savrasov, C. Humphreys, A. Sutton, Electron-energy-loss spectra and the structural stability of nickel oxide: an LSDA + U study, Phys. Rev. B 57 (3) (1998) 1505.
[45] J. Hölsä, M. Kirm, T. Laamanen, M. Lastusaari, J. Niittykoski, P. Novák, Electronic structure of the $Sr_2MgSi_2O_7$: Eu^{2+} persistent luminescence material, J. Lumin. 129 (12) (2009) 1560–1563.
[46] S. Shi, C. Ouyang, Q. Fang, J. Shen, W. Tang, C. Li, Electronic structure and magnetism of EuX (X = O, S, Se and Te): a first-principles investigation, EPL (Europhys. Lett.) 83 (6) (2008) 69001.
[47] M. Shishkin, G. Kresse, Self-consistent GW calculations for semiconductors and insulators, Phys. Rev. B 75 (23) (2007) 235102.
[48] F. Fuchs, J. Furthmüller, F. Bechstedt, M. Shishkin, G. Kresse, Quasiparticle band structure based on a generalized kohn-sham scheme, Phys. Rev. B 76 (11) (2007) 115109.
[49] J. Lee, A. Seko, K. Shitara, K. Nakayama, I. Tanaka, Prediction model of band gap for inorganic compounds by combination of density functional theory calculations and machine learning techniques, Phys. Rev. B 93 (11) (2016) 115104.
[50] P. Dorenbos, A review on how lanthanide impurity levels change with chemistry and structure of inorganic compounds, ECS J. Solid State Sci. Technol. 2 (2) (2013) R3001–R3011.
[51] P. Dorenbos, Modeling the chemical shift of lanthanide 4f electron binding energies, Phys. Rev. B 85 (16) (2012) 165107.
[52] P. Dorenbos, Lanthanide 4f-electron binding energies and the nephelauxetic effect in wide band gap compounds, J. Lumin. 136 (2013) 122–129.
[53] P. Dorenbos, Determining binding energies of valence-band electrons in insulators and semiconductors via lanthanide spectroscopy, Phys. Rev. B 87 (3) (2013) 035118.
[54] A. Egranov, T.Y. Sizova, R.Y. Shendrik, N. Smirnova, Instability of some divalent rare earth ions and photochromic effect, J. Phys. Chem. Solids 90 (2016) 7–15.
[55] R. Shendrik, A. Myasnikova, E. Radzhabov, A. Nepomnyashchikh, Spectroscopy of divalent rare earth ions in fluoride crystals, J. Lumin. 169 (2016) 635–640.
[56] H. Rüter, H.v. Seggern, R. Reininger, V. Saile, Creation of photostimulable centers in bafbr: Eu^{2+} single crystals by vacuum ultraviolet radiation, Phys. Rev. Lett. 65 (19) (1990) 2438.
[57] R. Shendrik, E. Radzhabov, Temperature dependence of Ce^{3+} and Pr^{3+} emission in CaF_2, SrF_2, and BaF_2, IEEE Trans. Nucl. Sci. 57 (3) (2010) 1295–1299.